ORIGINAL ARTICLE

Endoscopic Orientation of the Parasellar Region in Sphenoid Sinus with Ill-Defined Bony Landmarks: An Anatomic Study

Sameh M. Amin, M.D.,[1] Ashraf Y. Nasr, M.D.,[2] Hamid A. Saleh, M.D.,[4] Mohamed M. Foad, M.D.,[5] and Islam R. Herzallah, M.D.[3]

ABSTRACT

The sphenoid bony landmarks are important for endoscopic orientation in skull base surgery but show a wide range of variations. We aimed to describe an instructional model for the endoscopic parasellar anatomy in sphenoid sinuses with ill-defined bony landmarks. Five preserved injected cadaveric heads and four sides of dry skulls were studied endoscopically via transethmoid, transsphenoidal approach. The parasellar region was exposed by drilling along the maxillary nerve (V2) canal [the length of the foramen rotundum (FR) between the middle cranial fossa and the pterygopalatine fossa]. This was achieved by drilling in the inferior part of the lateral wall of posterior ethmoids immediately above the sphenopalatine foramen. Cavernous V2 was traced to the paraclival internal carotid artery (ICA). Cavernous sinus (CS) apex was exposed by drilling a triangle bounded by V2 and its canal inferiorly, bone between FR and superior orbital fissure (SOF) anteriorly, and ophthalmic nerve (V1) superiorly. Drilling was continued toward the annulus of Zinn (AZ) and optic nerve superiorly and over the intracavernous ICA posteriorly. Endoscopic measurements between V2, SOF, AZ, and opticocarotid recess were obtained. Endoscopic systematic orientation of parasellar anatomy is presented that can be helpful for approaching sphenoid sinus with ill-defined bony landmarks.

KEYWORDS: Cavernous sinus, parasellar, sphenoid, bony landmarks, endoscopic sinus surgery

The cavernous sinus (CS) is recently considered as part of the extradural neural compartment. The CS extends from the paraclinoid area posteriorly to the orbit apex anteriorly. Medially, it is related to the sphenoid sinus and laterally to the middle cranial fossa (MCF) dura.[1] Transsphenoidal endonasal endoscopic pituitary surgery has long been a standard technique, reaching state-of-the-art level. Increasing interest is now focused toward the parasagittal skull base, particularly the parasellar region. Many studies have been published describing the endonasal anatomy of the CS.[2–4] These studies tried to provide an anatomic model based on evident bony landmarks in the sphenoid sinus.[2–4] These bony landmarks are age-related, depend upon the degree of pneumatization of the sphenoid sinus, and show a wide range of incidence and variation.[5–8] Conchal and presellar

[1]ENT Department, Fayoum University, El Fayoum, Egypt, [2]Department of Anatomy, [3]ENT Department, Zagazig University, El Zagazig, Egypt, [4]Department of Anatomy, King Abd ElAziz University, Jeddah, Saudi Arabia, [5]Department of Neurosurgery, Cairo University, Cairo, Egypt.

Address for correspondence and reprint requests: Sameh M. Amin, M.D., 26 El Sheik Kamer Street, EL Daher 11271, Cairo, Egypt (e-mail: Samehamin@web.de).

Skull Base 2010;20:421–428.

Received: August 15, 2009. Accepted after revision: February 28, 2010. Published online: June 11, 2010.
DOI: http://dx.doi.org/10.1055/s-0030-1261262.
ISSN 1531-5010.

Table 1 Measurements in Medial Wall of the Parasellar Region

Measurements in the Medial Wall of the Parasellar Region	Minimum (mm)	Maximum (mm)	Mean Length (mm)	SD (mm)
OCR angle to center of AZ	12	16	12.85	1.2030
OCR to V2 decussating with ICA	18	23	20.35	1.7958
Vertical line from V2 canal to skull base passing of AZ	17	21	18.6	1.0488
V2 canal to center point of annulus of AZ	15	17	15.2	0.6325
V2 cavernous part (from FR at MCF side to ICA)	22	26	23.2	1.1353
V2 canal (FR from PPF to MCF side)	11	15.5	12.45	1.6064
V2 canal (FR at MCF side) to SOF	8	12	10.1	1.1005

AZ, annulus of Zinn; FR, foramen rotundum; ICA, internal carotid artery; MCF, middle cranial fossa; OCR, opticocarotid recess; PPF, pterygopalatine fossa; SOF, superior orbital fissure; V2, maxillary nerve.

sphenoid pneumatization make endoscopic transsphenoidal surgery less favorable. Accordingly, sphenoid bony landmarks cannot be used solely in a unified anatomic instructional model. The authors tried in this study to describe an endoscopic orientation that is relatively independent on the degree of sphenoid sinus pneumatization and its bony landmarks.

METHODS

The study was performed on 10 sides of five adult formaldehyde-preserved cadaveric heads injected with red latex and four sides of dry skulls. The dry skulls were used to help in planning the anatomic model. Measurements of bony dimensions were taken from both dry skulls and preserved cadavers, whereas soft tissue dimensions were taken from the preserved cadavers only.

Nasal endoscopes (Karl Storz and Co., Tuttlingen, Germany), 4 mm in diameter, 18 cm in length, with 0, 30, and 45 degrees, were used. Digital pictures were reproduced by coupling the endoscope to the video camera and using a computer capture system. A classic anterior ethmoidectomy, wide middle meatal antrostomy, complete posterior ethmoidectomy, and sphenoidectomy were performed, exposing the skull base. The posterior part of the bony septum was removed together with the intersphenoid septum. A vertical incision was performed in the posterior part of the middle meatus just behind the posterior fontanelle. A mucosal flap was elevated to expose the thick orbital process of the vertical plate of the palatine bone and its ethmoid crest. The sphenopalatine foramen (SPF) and the sphenopalatine artery (SPA) were then identified and carefully dissected. The caudal part of middle turbinate was excised to increase the operative field space.

Important bony landmarks, if possible, were identified in the sphenoid sinus. The sella floor, planum sphenoidale, tuberculum sellae, and clivus were identified in the midline. The internal carotid artery (ICA), optic nerve, opticocarotid recess (OCR), and occasionally the CS apex and V2 were identified in the lateral wall of the sphenoid sinus. The medial wall of the CS was dissected in a systematic, ordered fashion, and measurements were obtained from the medial wall of the parasellar region (Table 1). Studying the variable incidence of both sphenoid sinus pneumatization degree and sphenoid bony landmarks was outside the scope of this study and was not documented. Consequently, measurements were taken irrespective of the sphenoid sinus pneumatization type with no preselection.

RESULTS

The operative field included the lateral wall of the posterior ethmoid and sphenoid sinuses. The medial wall of parasellar region can be described endonasally in the form of a rectangular area bounded by cavernous V2 inferiorly, optic canal superiorly, a vertical line passing from center of annulus of Zinn (AZ) to foramen rotundum (FR) at the MCF side anteriorly, and the cavernous ICA posteriorly.

The Maxillary Nerve

In this study, the V2 canal is defined as the bony canal lying between the FR at the pterygopalatine fossa (PPF) and MCF. The V2 canal can be exposed directly by drilling the pterygoid base through the lateral wall of the inferior part of posterior ethmoids immediately above the SPF. At the PPF end of the FR, the V2 lies ~7 mm superolateral to the SPF.[9] Posterior drilling of the V2 canal was continued to the MCF side of the FR (see Fig. 2A). The length of the V2 canal (from the FR cranial side to the PPF) ranged from 11 to 15.5 mm with an average of 12.45 mm (Figs. 1A and B). Drilling medial to the V2 canal just behind the SPF was limited as much as possible in order not to injure the Vidian nerve, which may be as close to the V2 as 4 to 6 mm. The cavernous V2 was drilled out posteriorly to the paraclival ICA (Figs. 2B and 2C). The V2 may make a bony prominence in lateral wall of the hyperpneumatized sphenoid sinus, and in this case its exposure was relatively easier. However, even in the hypopneumatized sphenoid sinus, the V2 presented a guideline for the

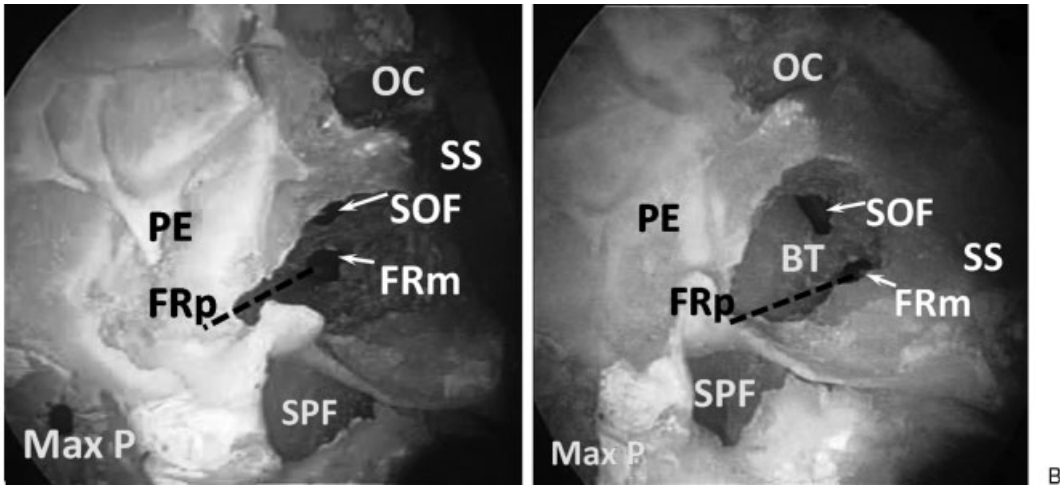

Figure 1 (A) Different areas of bone drilling. V2 canal (dashed line) lies between foramen rotundum at pterygopalatine (FRp) and foramen rotundum at middle cranial fossa (FRm). V2 canal extends through the lateral wall of the inferior part of posterior ethmoids immediately above the sphenopalatine foramen (SPF). FRm and V2 canal lie below the medial end of superior orbital fissure (SOF), and the anterior end of optic canal (OC) and annulus of Zinn lie superior to the medial end of SOF. (B) Bone trajectory (BT) separating SOF from FRm and V2 canal (dashed line). The wide distance between FRp and FRm suggests the V2 canal terminology. The OC inclines away from the skull base as it reaches the posterosuperior angle of posterior ethmoid sinus (PE). MAX P, posterior wall of maxillary sinus; SS, sphenoid sinus.

lower margin of the CS and paraclival ICA. The average length of the V2 from the FR at the PPF to the paraclival ICA was 35.65 mm.

Vertical Line from V2 Canal to Superior Orbital Fissure and AZ and Exposure of CS Apex

The vertical line that extends from the V2 canal toward the AZ passes through the medial end of the superior orbital fissure (SOF). The average distance from the V2 canal to the medial end of SOF and to the AZ was 10.1 and 15 mm, respectively (Table 1). The CS apex was exposed by drilling a bony triangle bounded by the V2 inferiorly, bone between FR and SOF anteriorly, and the V1 superiorly. The V2 canal presented an important landmark for the orbit apex and SOF, which lay 8 to 12 mm above the V2 canal (Fig. 1B).

The superior ophthalmic vein was constantly present in all specimens traversing the SOF above and parallel to the cavernousV2. This vein presented a limiting factor for drilling this bony area. In two specimens, an emissary vein traversing the V2 canal joined the superior ophthalmic vein (Fig. 2B). Adipose tissue between V1 and V2 was occasionally present and originated from the SOF. Adipose tissue when present obscured V1 and presented less limitation for drilling (Figs. 2A, 3A, and 3B).

The Optic Nerve

Bone drilling was then continued superiorly toward the optic nerve. The latter starts at the AZ and passes posteromedially in the lateral wall of the sphenoid sinus and/or Onodi cell to reach the OCR. The length of the optic nerve from the center of the AZ to the OCR was 13 mm on average. From the OCR to the AZ, the nerve inclined gradually inferiorly away from the skull base (Figs. 1B and 2C). As a result, the distance from V2 (at its decussation with ICA) to the OCR was a mean of 20.35 mm, and that from the V2 canal to the center point of the AZ was only 15.2 mm on average (Table 1).

The Medial Wall of the CS

After exposure of the FR and SOF and drilling the trajectory of bone between them, the rest of the lateral wall of the sphenoid sinus was removed anteroposteriorly toward the cavernous ICA. This led to exposure of the medial wall of the CS formed by the outer layer of the dura. The latter was cut to expose different cranial nerves. These neural structures can be divided for practical purposes by an imaginary line into motor and sensory triangles (Fig. 2D). This line extends from the point of decussation of V2 and paraclival ICA posteroinferiorly to the AZ anterosuperiorly. The motor triangle above this line contains the oculomotor (III), trochlear (IV), and abducent (VI) nerves, in addition to the inferolateral and meningohypophyseal trunks arising from the intracavernous ICA and giving blood supply to these nerves.[10] The abducent nerve is the most superficial, the oculomotor superior to it and at deeper level. The trochlear nerve is situated at a deeper level, lower to the oculomotor and parallel to the abducent, so that visualization of the trochlear is achieved only after downward traction of the abducent. The abducent nerve can be traced posteriorly a few millimeters just above the

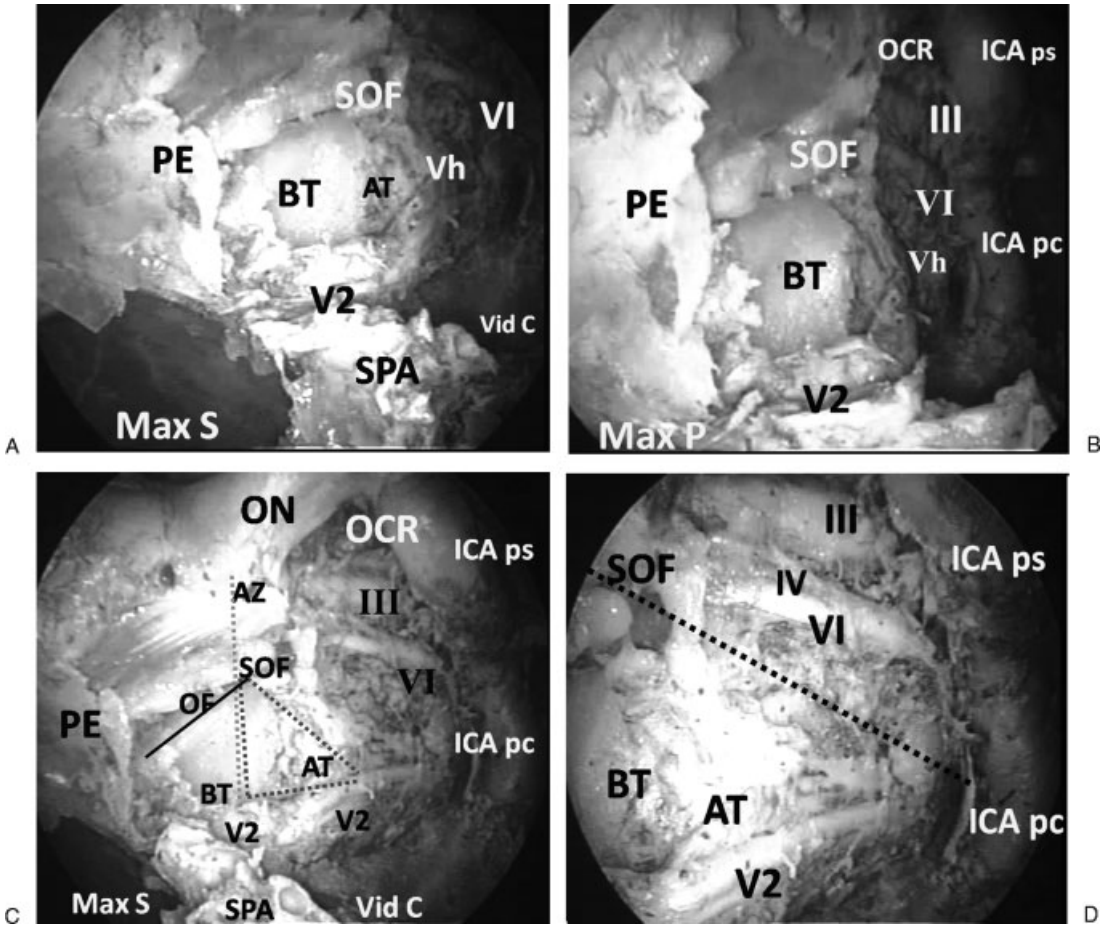

Figure 2 (A) Endoscopic view of right maxillary nerve (V2) after drilling its canal superolateral to cut sphenopalatine artery (SPA). The superior orbital fissure (SOF) and orbital apex become more evident. Adipose tissue (AT) is partially obscuring a huge vein (Vh), superior ophthalmic vein (SOV), above V2. The maxillary sinus (Max S) posterior wall and remnant of posterior ethmoid sinus (PE) appear intact showing that the pterygopalatine fossa is not violated. A bone trajectory (BT) separates V2 canal from SOF at the cavernous sinus apex. Vidian canal (Vid C) protuberance appears in the floor of sphenoid sinus. Abducent nerve (VI) appears in anterior part of the medial wall of cavernous sinus. (B) Endoscopic view of V2 in its canal in relation to the medial wall of parasellar region. After removal of adipose tissue above V2, a huge vein (Vh), namely the SOV, appears originating from SOF and passing parallel to V2. A small tributary accompanying V2 in its canal is joining SOV. The occulomotor (III) and abducent (VI) nerves emerge laterally to the parasellar internal carotid artery (ICA ps) and pass anteriorly toward the SOF. Posteriorly, the cavernous internal carotid artery (ICA) extends downward from opticocarotid recess (OCR) as parasellar (ICA ps) and paraclival (ICA pc) segments. (C) Endoscopic view showing the four sides of the approach. V2 inferiorly, optic nerve (ON) in its dural sheath superiorly, and cavernous ICA posteriorly, which extends from opticocarotid recess (OCR) to V2 decussation with ICA. The cavernous ICA is formed by a C shaped parasellar segment (ICA ps) and a vertical paraclival segment (ICA pc). The anterior side is shown with a vertical dashed line passing through annulus of Zinn (AZ), SOF, bone trajectory between SOF and V2, and its canal. After removal of bone covering the medial wall of parasellar region and dura forming the medial of cavernous sinus, the abducent (VI) and occulomotor (III) nerves can be seen in the cavernous sinus apex anteriorly. Posteriorly, these nerves lie lateral to the ICA ps. AT above V2 obscures ophthalmic nerve (V1). The Vid C appears in the floor of sphenoid sinus and passes anterolateral to SPA and foramen, where it is very close to V2. The posterior wall of Max) appears anterior to V2 canal. The cavernous sinus apex is exposed by drilling a bony dashed triangle limited by V2 and its canal inferiorly, V1 posterolaterally, and BT between SOF and V2 canal anteriorly. This BT becomes narrower anteriorly due to downward slope of orbital floor (OF) (continuous line) anteriorly, favoring a mediolateral approach to SOF. (D) Endoscopic view showing nerves in the medial wall of right cavernous sinus. The medial wall of cavernous sinus is divided by a dashed line into motor and sensory triangles. In the motor triangle (top) the abducent nerve (VI) is the most superficial, and the occulomotor (III) is superior and parallel to VI and at a deeper level. The trochlear nerve is barely seen deep and parallel to VI and inferior to III. The sensory triangle (bottom) contains V2 and AT, which obscures a huge SOV and ophthalmic nerve (V1) at a deeper lateral level.

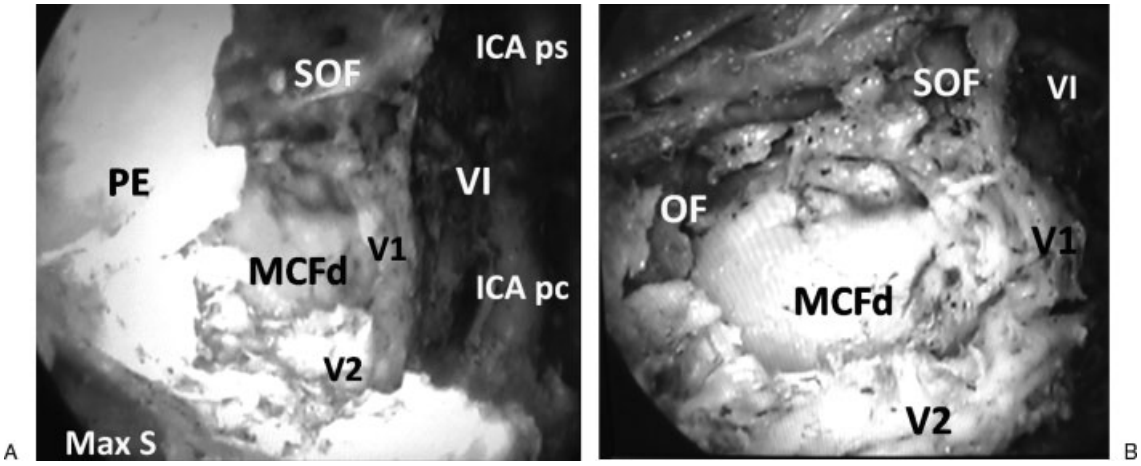

Figure 3 (A) Endoscopic view showing right cavernous sinus apex. The bone trajectory between V2 canal and superior orbital fissure (SOF) is drilled in addition to bone of middle cranial fossa (MCF) inferomedial to ophthalmic nerve (V1). The posterior ethmoid (PE) and maxillary sinus (Max S) limit the approach laterally. Medially, the abducent nerve (VI) appears as the most superficial nerve in the medial wall of cavernous sinus. The parasellar (ICA ps) and paraclival (ICA pc) segments of cavernous internal carotid artery limit the approach medially. (B) Endoscopic view showing the orbital floor (OF) slopes toward anterior end of V2 canal at PPF. The MCF dura (MCF d) appears between V1 and V2. Abducent nerve (VI) appears lateral and superior to V1, which branches before entering SOF.

decussation of V2 with the paraclival segment of the ICA. In the midcavernous area, the nerve lies lateral to the lower horizontal segment of the parasellar ICA. Anteriorly, the abducent nerve crosses inferior to the oculomotor at the SOF. The sensory triangle contains the superior ophthalmic vein above V2 in addition to adipose tissue (Fig. 2D). Deeper and more laterally lies the V1, which branches at variable distances before entering the SOF (Figs. 3A and B).

The Cavernous ICA

This side of the operative field is defined between the OCR and the point where the cavernous V2 decussates with the paraclival ICA. The distance between these two landmarks was 20.35 mm on average. This distance does not reflect the actual length of looping/bending intracavernous ICA, but rather, the bone needed to be removed to expose the intracavernous ICA. After exposure of the previously mentioned landmarks and drilling of the lateral wall of the sphenoid sinus, the cavernous ICA can be exposed by removing the overlying bone with possible extension to the sellar floor. The intracavernous ICA is formed of parasellar and paraclival segments (Figs. 2B and C). The parasellar segment is C-shaped, related laterally to the sella, and is formed of the upper and lower horizontal segments with the anterolateral bend. The paraclival segment is vertically oriented.

DISCUSSION

The bony landmarks in the sphenoid sinus are crucial for endoscopic orientation in skull base surgery. Pneumatization of the sphenoid sinus is usually classified into three categories: conchal, presellar, and sellar/postsellar types. There is discrepancy in literature between degree of pneumatization of the sphenoid sinus and the incidence of bony landmarks. The presence of well-pneumatized sphenoid sinus does not ensure clear bony surgical landmarks.[6] Preoperative radiological identification of sphenoid bony landmarks is not essentially associated with intraoperative endoscopic visualization.[5] Navigational devices can be used to confirm surgical landmarks in hypopneumatized and well-pneumatized sphenoid sinus with ill-defined bony landmarks. Surgical navigation accuracy is best reported as target registration error, which is probably in the 1.5- to 2.0-mm range. However, a wider range of mean error of registration is reported.[11]

Alfieri et al[2] described the endoscopic anatomy of the parasellar region depending upon the sphenoid bony landmarks. The feasibility of the approach is questioned for hypopneumatized and septated sphenoid. Similarly, Frank and Pasquini[4] described an endoscopic ethmoido-pterygo-sphenoidal (EPS) approach, which was basically an extended transsphenoidal approach. Despite designing the EPS approach for anterior exposition of the CS, the CS apex anatomy was not specified and the transpterygoid component of the approach was saved for tumors invading the lateral sphenoid recess and lateral compartment of CS.

V2 represented in this study the lower margin of the parasellar region. V2 offers an excellent orientation for the parasellar region owing to its multiangled mediolateral/posteroanterior direction at the skull base.[12] It presents also a landmark for the paraclival ICA posteriorly and for the CS apex, SOF, and AZ anteriorly. More

anteriorly, V2 leads invariably to the PPF. There is a tendency in the literature toward refinement of V2 exposure at the skull base. Sabit et al[13] proposed exposure of the inferior orbital nerve, dissection of the PPF, and retraction of the SPA to expose the FR. Herzallah et al[12] proposed removing a small strip of bone from the posterior wall of the maxillary sinus just lateral to and above the SPF. Fortes et al[14] suggested retrograde dissection of the SPA to identify the internal maxillary artery and hence V2 in a deeper plane. The authors present a new technique that directly exposes V2 and bypasses the vascular PPF compartment. The localized drilling of the upper part of pterygoid base, needed only for exposure of V2, avoids entering the PPF, which rich in neural and vascular components.[13] Various endoscopic measurements between the V2, SOF, AZ, and OCR were obtained and reported.

Regarding the endoscopic anatomy of the parasellar region, this study provides a new description of V2 into two parts: one inside its canal (V2 canal) and the second, the cavernous V2. The V2 canal was used as an important guideline to the SOF and CS apex. In addition, the authors divided the medial wall of the CS into sensory and motor triangles. This is partly in agreement with the Pittsburgh group, which recommended no manipulation above the upper border of V2 to avoid abducent nerve injury.[15] Last, different measurements were taken in the parasellar region and are highlighted in this anatomic study.

In this study, we advocated exposure of the CS apex by drilling the bone between the V2 canal and SOF. This trajectory of bone was ~10 mm in length. Sabit et al[13] offered anterior exposure of the CS apex through a transmaxillary approach by drilling the bone of the posterior wall of PPF superior and medial to FR to open the SOF. In comparison to our anatomic model, the distance between the FR and SOF anteriorly in the PPF was narrower, and dissection of the highly vascular PPF was mandatory to expose the FR at the PPF side. In addition, great care was needed not to drill the orbital floor through this narrow field to avoid fat herniation. The main limiting factor in our approach is the presence of the superior ophthalmic vein above V2 and the occasional finding of adipose body between V1 and V2.[1] The superior ophthalmic vein has different locations within the SOF according to the morphology of SOF.[16] Adipose tissue between V1 and V2 was also reported in other studies, but presented less limitation for dissection.[1,2]

In real surgery, the dura of the medial wall of CS can be opened after localization of cavernous ICA with endonasal Doppler or other navigation system.[4] In this study, the CS is divided for practical purposes into sensory and motor triangles. The authors think that this division will also help the skull base surgeon avoid injury of motor nerves or their blood supply.

Our anatomic model is primarily extradural. It can be extended anteriorly to PPF, orbital apex, or posteriorly to the sellar region. It depends upon systematic, ordered bony drilling and is relatively independent upon the degree of pneumatization of the sphenoid sinus or its bony landmarks. It allows anterior exposition of the parasellar region so that angled distorted endoscopic views are minimized. One disadvantage of this study was the use of formalin-preserved cadavers. Fresh frozen cadavers are associated with better and more realistic handling of tissue planes. However, most of our dissection was bony drilling and extradural. In addition, the use of injected cadavers allowed for identification of important vascular structures including arteries and veins.

CONCLUSION

The results of this study might provide the endoscopic sinus and skull base surgeon with a better understanding of endoscopic orientation and dimensions of the parasellar region in sphenoid sinus with ill-defined bony landmarks.

REFERENCES

1. Dolenc V. Surgical triangles of the cavernous sinus. In: Dolenc V, ed. Anatomy and Surgery of the Cavernous Sinus. Wien, New York: Springer-Verlag; 1989:7–29
2. Alfieri A, Jho HD. Endoscopic endonasal cavernous sinus surgery: an anatomic study. Neurosurgery 2001;48:827–836; discussion 836–837
3. Bassim MK, Senior BA. Endoscopic anatomy of the parasellar region. Am J Rhinol 2007;21:27–31
4. Frank G, Pasquini E. Approach to the cavernous sinus. In: De Divitis E, Cappabianca P, eds. Endoscopic Endonasal Transsphenoidal Surgery. Wien, New York: Springer; 2003: 159–171
5. Hamid O, El Fiky L, Hassan O, Kotb A, El Fiky S. Anatomic variation of the sphenoid sinus and their impact on trans-sphenoid pituitary surgery. Skull Base 2008;18: 9–15
6. Kazkayasi M, Karadeniz Y, Arikan OK. Anatomic variations of the sphenoid sinus on computed tomography. Rhinology 2005;43:109–114
7. Reittner P, Doerfler O, Goritschnig T, et al. Magnetic resonance imaging patterns of the development of the sphenoid sinus: a review of 800 patients. Rhinology 2001;39: 121–124
8. Rice DH, Schaefer SD. Anatomy of the paranasal sinuses. In: Rice DH, Schaefer SD, eds. Endoscopic Paranasal Sinus Surgery. 3rd ed. Philadelphia: Lippincott Williams & Wilkins; 2004:48–49
9. Isaacs SJ, Goyal P. Endoscopic anatomy of the pterygopalatine fossa. Am J Rhinol 2007;21:644–647
10. d'Avella E, Tschabitscher M, Santoro A, Delfini R. Blood supply to the intracavernous cranial nerves: comparison of the endoscopic and microsurgical perspectives. Neurosurgery 2008;62(5, Suppl 2):ONS305–ONS310; discussion ONS310–ONS311

11. Citardi MJ, Batra PS. Intraoperative surgical navigation for endoscopic sinus surgery: rationale and indications. Curr Opin Otolaryngol Head Neck Surg 2007;15:23–27
12. Herzallah IR, Elsheikh EM, Casiano RR. Endoscopic endonasal study of the maxillary nerve: a new orientation. Am J Rhinol 2007;21:637–643
13. Sabit I, Schaefer SD, Couldwell WT. Extradural extranasal combined transmaxillary transsphenoidal approach to the cavernous sinus: a minimally invasive microsurgical model. Laryngoscope 2000;110(2 Pt 1):286–291
14. Fortes FS, Sennes LU, Carrau RL, et al. Endoscopic anatomy of the pterygopalatine fossa and the transpterygoid approach: development of a surgical instruction model. Laryngoscope 2008;118:44–49
15. Kassam AB, Prevedello DM, Carrau RL, et al. The front door to Meckel's cave: an anteromedial corridor via expanded endoscopic endonasal approach- technical considerations and clinical series. Neurosurgery 2009;64(3 Suppl):71–82; discussion 82–83
16. Reymond J, Kwiatkowski J, Wysocki J. Clinical anatomy of the superior orbital fissure and the orbital apex. J Craniomaxillofac Surg 2008;36:346–353